# Ellipsometry Study on thickness gradient silicon nitride (SiNx) film by plasma-enhanced chemical vapor deposition

**Qin Zhi Zhong**
University of Electronic Science and Technology of China https://orcid.org/0000-0003-2956-5921
**Xiang Luo** ( 2020222021519@std.uestc.edu.cn )
University of Electronic Science and Technology of China https://orcid.org/0000-0001-9194-0046
**Li Zhou**
University of Electronic Science and Technology of China
**Fu Shi Hu**
Chendu Tepin Electronic Technology Co. , Ltd
**Ping Li Dai**
University of Electronic Science and Technology of China
**Ya Shu Wang**
University of Electronic Science and Technology of China
**Peng Shao Yang**
University of Electronic Science and Technology of China

**Research Article**

**Keywords:** SiNx, thickness gradient, PECVD, process parameter ellipsometry

**Posted Date:** March 21st, 2022

**DOI:** https://doi.org/10.21203/rs.3.rs-1427374/v1



**Version of Record:** A version of this preprint was published at Optical and Quantum Electronics on January 11th, 2023. See the published version at https://doi.org/10.1007/s11082-022-04270-x.

# Abstract

As passivation layer and anti-reflection layer, silicon nitride (SiNx) thin film has been widely used in photovoltaic devices such as solar cells. The structure of SiNx film with thickness gradient can make full use of different wavelengths of sunlight. In this paper, we have studied this structure for the first time. While introducing a quartz layer by plasma-enhanced chemical vapor deposition (PECVD), we obtained a thin SiNx film in the center and gradually thicker toward the edge. The effects of PECVD process parameters, including deposition time, RF power, dielectric layer thickness, etc. on the thickness gradient of SiNx thin film are systematically studied. The film composition changing in the radial direction is also analyzed by ellipsometry. This study provides an instructive method for controlling the thickness gradient of SiNx films and plays an important role in using this structure to the solar cell application.


# 1. Introduction

With high density, good optical properties, thermal stability, and stable chemical properties(Mandracci et al. 2016; Merle and Goken 2011; Riley 2000), silicon nitride (SiNx) has been widely used in the fields of integrated circuit manufacturing(Habraken and Kuiper 1994), solar cells(El Amrani et al. 2008), micro-electro-mechanical systems (MEMS) devices(Kaushik et al. 2005), and so on. SiNx film is an effective passivation layer and anti-reflection layer for the solar cell application. Studies have shown that the conversion efficiency of the solar cells significantly improved after depositing SiNx film(Kishore et al. 1997; Lee et al. 2015; Richter et al. 2017; Zhong et al. 2016a).

However, so far, only uniform thickness of SiNx film was reported for the solar cell application. This uniform film will lead to the absorbance of a single wavelength of sunlight. Due to the uneven distribution of wavelength and energy in the solar spectrum, there are differences in the optimal thickness of transmission film for the different wavelengths of sunlight. Suppose the thickness of SiNx film can be controlled in the step state which is thin in the middle, and thick around, in other words, it shows thickness gradient. In that case, the light absorption can be further effectively increased, even the full transmission of solar spectrum is possibly realized by accurately controlling the film thickness and gradient, leading to greatly improve the performance of the fabricated optoelectronic devices. Therefore, how to effectively control the thickness gradient growth of SiNx thin film is of great significance to improve solar energy conversion efficiency. However, this structure has not been reported yet.

Although SiNx films can be grown by different methods, such as plasma-enhanced chemical vapor deposition (PECVD)(Tong et al. 2017; Wan et al. 2013; Zhang et al. 1996; Zhong et al. 2016b), atmosphere pressure CVD(Lelievre et al. 2019; Nowling et al. 2002), and magnetron sputtering(Kim and Chung 1998; Signore et al. 2012). In the solar cell area, as an antireflection layer, SiNx is usually deposited by PECVD due to its tunable refractive index in combination with excellent levels of surface and bulk passivation. Many photovoltaic researchers choose microwave PECVD system(Tong et al. 2017; Wan et al. 2013; Zhang et al. 1996; Zhong et al. 2016b). It is found that the structure and composition of SiNx films deposited in PECVD equipment with different compositions and temperatures are quite

different, resulting in different refractive index or Si/N ratio of the films. Guler etc. reported that the refractive index was linearly and positively correlated with the SiH4/(NH3 + SiH4)(Guler 2019). Kovacevic etc. summarized the reaction path of producing SiNx thin film with silane and ammonia gas, and concluded that various derivatives such as disilane and aminosilane produced by high-energy decomposition of silane and ammonia gas were precursors for depositing SiNx thin film(Kovacevic and Pivac 2017).

In this work, we present the growth of SiNx thin film with thickness gradient from the center to the edge by PECVD method by introducing a quartz dielectric layer. The influence of deposition time (*t*), RF power (*w*) and dielectric layer thickness (*d*) on the thickness gradient of SiNx thin films were studied by ellipsometry. The growth principle of SiNx thin film with thickness gradient was explored, and the control method of depositing SiNx thin films with a certain thickness gradient was obtained. By measuring the radial refractive index of the film, the composition changing of SiNx film with different thicknesses was studied.

# 2. Experimental Detail

After a standard chemical cleaning, $SiN_x$ films were prepared on 3-inch n-type Si substrate by low frequency PECVD system( 110 kHz, Trion) using Ar diluted $SiH_4$, $NH_3$ and $N_2$ as precusors. A quartz larger than the substrate was placed between the substrate and PECVD bottom electrode during the deposition process. The schematic figure is shown in Fig. 1. We mainly changed deposition time, power, and dielectric layer thickness to investigate the influence of these parameters on the thickness gradient. Deposition time(*t*) was 400s, 500s, and 600s, respectively. RF power(*w*) ranged from 80W to 120W. The thickness of dielectric layer(*d*) was 0.5mm, 1mm, and 2mm, respectively. While the temperature (T = 200℃) and all the other related deposition parameters (pressure 80pa, $SiH_4$ 250sccm, $NH_3$ 40sccm, $N_2$ 200sccm) were kept constant.

Ellipsometer (SENTECH SE850) was employed to obtain the thickness of samples at different positions in the diameter direction. To compare the composition variation at the different positions, we chose the refractive index of SiNx film at the incident wavelength of 632.8 nm.

# 3. Results And Discussion

In order to illustrate the influence of quartz layer on the deposition effect of SiNx film, we deposited two samples using the same process parameters for 500s. One sample was introduced a quartz as shown in Fig. 1. Another one was a referential sample. Silicon substrate was directly placed on PECVD bottom electrode without any quartz layer. Figure 2a shows $SiN_x$ sample after introducing quartz layer, obviously displaying rectangular isochromatic stripes. Different colors in the film represent the corresponding film thickness (Seo et al. 2014). However, the sample without quartz layer demonstrates homogeneous color, indicating uniform thickness. Figure 2c shows the thickness comparison at the different positions along the radial direction. We can clearly notice that the sample with quartz layer presents a characteristic of thickness gradient, showing thin thickness in the center, and thick thickness around comparatively. Also,

the thickness of SiNx film with thickness gradient are significantly smaller than that of without quartz layer at any corresponding position, and this difference is becoming smaller as closer to the edge. This work shows that $SiN_x$ thin film with thickness gradient can be obtained after introducing dielectric layer into PECVD deposition system.

# 3.1 Effect of deposition time on thickness gradient of SiNx thin films

In order to investigate the influence of different deposition time on various characteristic data of $SiN_x$ thin film with thickness gradient, we singly changed the deposition time to be 400s, 500s, and 600s, respectively, while kept the other process parameters constant. Except the above mentioned, RF power was 80W and dielectric thickness was 1mm.

Figure 3a displays the thickness of the different position for the three samples. It can be seen that the thickness shows symmetrical distribution along the center of the samples, and gradually increases from the center to the periphery. This indicates that the deposition rate also gradually increases from the center to the edge, and the deposition rates of thin films in the central area are about 0.29 nm/s, 0.31 nm/s and 0.32 nm/s for the samples 400s, 500s, and 600s, respectively. It was surprisingly found that the film thickness can be approximately fitted as a power function along the radial direction, which may be explained by the radial diffusion of reactants. The partial voltage of the quartz dielectric layer leads to reduce the peak electric field in the central area, and resultantly reducing the ionization rate of the process gas. With the decrease of gas ionization rate in area of the quartz dielectric layer, the concentration of reaction precursors is the minimum in the center, and gradually increases to the outside, thus results in thickness gradient of the deposited SiNx film, as shown in Fig. 3a. To clearly compare the influence of different deposition time on the thickness distribution of SiNx thin films, we normalized the film thickness based on the minimum value. The result of the normalized thickness distribution is shown in Fig. 3b. It can be clearly seen that the three normalized thickness curves in the radial direction are almost repetitive. This may be due to the inhomogeneous growth of SiNx film with time for the certain position, and the concentration difference of reactants in the reaction chamber is time independent (Smietana et al. 2011).

# 3.2 Influence of RF Power on Thickness Gradient of SiNx Film

Figure 4a shows the thickness variation for the $SiN_X$ films deposited with the different RF power from 80W to 100W. The film thickness of these three samples also shows gradual increase from the center to the edge, showing the characteristics of thin center area and thick edge area.

From Fig. 4a, it can be seen that the film thickness increases gradually with the increasing of deposition power. The deposition rates are calculated to be 0.29 nm/s, 0.32 nm/s and 0.37 nm/s, respectively, and the deposition rate at the edge of 120W deposited sample reaches 0.97 nm/s. The increase in deposition rate is related to the increasing of plasma concentration with change of RF power(Zhang et al. 1996). But

this value is still lower than that of traditional uniform thin film with power of 80W, as shown in Fig. 2b, who's the deposition rate is 0.99 nm/s. We ascribe this to the significant decreasing of RF bias because of the dielectric layer. As we can see, the right values are larger than the left ones, this may be caused by that the measurement points are not strictly symmetrical.

In order to study the effect of RF power on the thickness gradient, we normalized the radial thickness data based on the minimum value, and the radial distribution of film thickness is shown in Fig. 4b. We notice that the gradient for the 80W deposited $SiN_X$ is the smallest, while the gradient of the other two samples is almost same. That is to say, when the RF power increases to be a certain value, with the increasing of RF power, the deposition rate will increase, but it has no obvious effect on the radial film thickness gradient. This phenomenon should be related to the radial concentration difference of precursors in the chamber but needs to be further explored.

## 3.3 The Influence of different dielectric layer thickness on thickness gradient of $SiN_X$ film

In the process of capacitively coupled gas discharge, the partial voltage of the dielectric layer will reduce the longitudinal electric field, which will affect the ionization rate of gas molecules and the deposition rate of thin films. Therefore, in the actual production process, the gas discharge process can be influenced by selecting the suitable dielectric layer, so that it is easier to control various characteristic parameters of the thin film(Kawamura et al. 2017).

Figure 5a shows the thickness changing for the $SiN_X$ films deposited using the different dielectric layer with the thickness 0.5mm, 1mm, and 2mm, respectively. We can clearly see the deposition rate dramatically increases with decreasing dielectric layer thickness. The deposition rates of central area are 0.19nm/s, 0.29nm/s, and 0.46nm/s for three samples. This variation is because partial bias falls on the dielectric layer. It is more obvious in the thicker dielectric layer, which reduces the space electric field, leading to a decrease in the ionization rate of process gas and the concentration of precursors required for film formation, thus reducing the deposition rate of SiNx films with the increasing of the dielectric layer.

Figure 5b displays the normalized curves for the three samples. The edge thickness of the film is 2.4 times more than the thickness of the central area when the dielectric layer is 2mm, and 1.5 times when the dielectric layer is 0.5 mm in thickness. Therefore, the thickness gradient of the SiNx film can increase with the increase of the dielectric layer thickness, and shows the tendency of sacrificing the deposition speed for a larger film thickness gradient. Xu, etal reported the introduction of dielectric layer leads to uneven distribution of reaction precursors, which will lead to radial diffusion [13]. Therefore, it can be speculated that using a thicker dielectric layer will lead to a greater radial concentration difference of aminoalkane precursors and enhance radial diffusion, thus leading to a greater thickness gradient of SiNx film.

## 3.4 Refractive index radial variation of SiNx thin films with gradient thickness

Figure 6 depicts the refractive index variation along the radial direction for a typical $SiN_x$ film. The results show a tendency to increase gradually from the center to the edge. Generally speaking, the refractive index of SiNx films is mainly linearly related to the silicon/nitrogen ratio and atomic density(Gardeniers et al. 1996). The refractive index of SiNx film is almost stable at 1.86 in the range of 1.5cm in radius. In this range, the refractive index difference of SiNx films has little change due to the small change in thickness. When the radius reaches from 1.5 cm to 3.5 cm, the refractive index increases from 1.85 to 1.98. This should be caused by increasing silicon/nitrogen ratio along with radial direction.

# 4. Conclusion

In this work, SiNx thin films with thickness gradients were deposited at low temperature(200℃) in a PECVD deposition system with ammonia and silane as reaction gases. The effects of deposition time, radio frequency power, and dielectric layer thickness on the thickness gradient of SiNx thin films were systematically studied by ellipsometry. Results show that the thickness of the dielectric layer has the greatest influence on the thickness gradient compared to the other two factors. Also, the ratio of silicon to nitrogen in thin films was obtained by analyzing the change of radial refractive index. Our work suggests that introducing of dielectric layer is a promising simple approach to obtain $SiN_x$ antireflection and passivation layer with thickness gradient, and can be further extended to optoelectronics, to achieve a wide range of next-generation low-cost high-efficiency devices.

# Declarations


### Acknowledgments

This work was financially supported by the Science and Technology Department of Sichuan Province (2020YFG0042) and the Foundation of State Key Laboratory of Electronic Thin Films and Integrated Devices (kFJJ201911).


**Conflict of Interest:** The authors declare that they have no conflict of interest.

# References


1. El Amrani, A., Menous, I., Mahiou, L., Tadjine, R., Touati, A., Lefgoum, A.: Silicon nitride film for solar cells. Renew. Energy. **33**, 2289–2293 (2008). https://doi.org/10.1016/j.renene.2007.12.015
2. Gardeniers, J.G.E., Tilmans, H.A.C., Visser, C.C.G.: LPCVD silicon-rich silicon nitride films for applications in micromechanics, studied with statistical experimental design. J. Vac Sci. Technol. A. **14**, 2879–2892 (1996). https://doi.org/Doi 10.1116/1.580239

3. Guler, I.: Optical and structural characterization of silicon nitride thin films deposited by PECVD. Mater. Sci. Eng. B-Advanced Funct. Solid-State Mater. **246**, 21–26 (2019). https://doi.org/10.1016/j.mseb.2019.05.024
4. Habraken, F.H.P.M., Kuiper, A.E.T.: Silicon-Nitride and Oxynitride Films. Mater. Sci. Eng. R-Reports. **12**, 123–175 (1994). https://doi.org/Doi 10.1016/0927-796x(94)90006-X
5. Kaushik, A., Kahn, H., Heuer, A.H.: Wafer-level mechanical characterization of silicon nitride MEMS. J. Microelectromechanical Syst. **14**, 359–367 (2005). https://doi.org/10.1109/JMEMS.2004.839315
6. Kawamura, E., Wen, D.Q., Lieberman, M.A., Lichtenberg, A.J.: Effect of a dielectric layer on plasma uniformity in high frequency electronegative capacitive discharges. J. Vac. Sci. Technol. A. 35, (2017). https://doi.org/Artn 05c31110.1116/1.4993595
7. Kim, J.H., Chung, K.W.: Microstructure and properties of silicon nitride thin films deposited by reactive bias magnetron sputtering. J. Appl. Phys. **83**, 5831–5839 (1998). https://doi.org/10.1063/1.367440
8. Kishore, R., Singh, S.N., Das, B.K.: Screen printed titanium oxide and PECVD silicon nitride as antireflection coating on silicon solar cells. Renew. Energy. **12**, 131–135 (1997). https://doi.org/Doi 10.1016/S0960-1481(97)00030-X
9. Kovacevic, G., Pivac, B.: Reactions in silicon-nitrogen plasma. Phys. Chem. Chem. Phys. **19**, 3826–3836 (2017). https://doi.org/10.1039/c6cp05395e
10. Lee, E.G., Kim, J.H., Ko, H., Kim, C.Y.: The anti-reflection coating using the silicon nitride and silicon monoxide for InP based solar cells. J. Comput. Theor. Nanosci. **12**, 871–874 (2015). https://doi.org/10.1166/JCTN.2015.3819
11. Lelievre, J.F., Kafle, B., Saint-Cast, P., Brunet, P., Magnan, R., Hernandez, E., Pouliquen, S., Massines, F.: Efficient silicon nitride SiNx:H antireflective and passivation layers deposited by atmospheric pressure PECVD for silicon solar cells. Prog. Photovoltaics. **27**, 1007–1019 (2019). https://doi.org/10.1002/pip.3141
12. Mandracci, P., Frascella, F., Rizzo, R., Virga, A., Rivolo, P., Descrovi, E., Giorgis, F.: Optical and structural properties of amorphous silicon-nitrides and silicon-oxycarbides: Application of multilayer structures for the coupling of Bloch Surface Waves. J. Non Cryst. Solids. **453**, 113–117 (2016). https://doi.org/10.1016/j.jnoncrysol.2016.10.002
13. Merle, B., Goken, M.: Fracture toughness of silicon nitride thin films of different thicknesses as measured by bulge tests. Acta Mater. **59**, 1772–1779 (2011). https://doi.org/10.1016/j.actamat.2010.11.043
14. Nowling, G.R., Babayan, S.E., Jankovic, V., Hicks, R.F.: Remote plasma-enhanced chemical vapour deposition of silicon nitride at atmospheric pressure. Plasma Sources Sci. Technol. **11**, 97–103 (2002). https://doi.org/10.1088/0963-0252/11/1/312
15. Richter, A., Benick, J., Feldmann, F., Fell, A., Hermle, M., Glunz, S.W.: n-Type Si solar cells with passivating electron contact: Identifying sources for efficiency limitations by wafer thickness and resistivity variation. Sol. Energy Mater. Sol. Cells. **173**, 96–105 (2017). https://doi.org/10.1016/J.SOLMAT.2017.05.042

16. Riley, F.L.: Silicon nitride and related materials. J. Am. Ceram. Soc. 83, 245–265 (2000). https://doi.org/DOI 10.1111/j.1151-2916.2000.tb01182.x
17. Seo, H., Sakai, T., Ohtake, H., Furuta, M.: Stacked Organic Photoconductive Films and Thin-Film Transistor Circuits Separated by Thin Silicon Nitride for a Color Image Sensor. 2014 Ieee Sensors. 1672–1675 (2014)
18. Signore, M.A., Sytchkova, A., Dimaio, D., Cappello, A., Rizzo, A.: Deposition of silicon nitride thin films by RF magnetron sputtering: a material and growth process study. Opt. Mater. (Amst). **34**, 632–638 (2012). https://doi.org/10.1016/J.OPTMAT.2011.09.012
19. Smietana, M., Bock, W.J., Szmidt, J.: Evolution of optical properties with deposition time of silicon nitride and diamond-like carbon films deposited by radio-frequency plasma-enhanced chemical vapor deposition method. Thin Solid Films. **519**, 6339–6343 (2011). https://doi.org/10.1016/j.tsf.2011.04.032
20. Tong, J., To, A., Lennon, A., Hoex, B.: Unintentional consequences of dual mode plasma reactors: Implications for upscaling lab-record silicon surface passivation by silicon nitride. Jpn J. Appl. Phys. **56**, 08MB12 (2017). https://doi.org/10.7567/JJAP.56.08MB12/XML
21. Wan, Y., McIntosh, K.R., Thomson, A.F.: Characterisation and optimisation of PECVD SiNx as an antireflection coating and passivation layer for silicon solar cells. AIP Adv. **3**, 032113 (2013). https://doi.org/10.1063/1.4795108
22. Zhang, X., Ding, K., Yang, A., Shao, D.: Processing and Characterisation of PECVD silicon nitride films. Adv. Mater. Opt. Electron. **6**, 147–150 (1996). https://doi.org/10.1002/(sici)1099-0712(199605)6:3<147::aid-amo227>3.3.co;2-7
23. Zhong, Z., Li, Z., Gao, Q., Li, Z., Peng, K., Li, L., Mokkapati, S., Vora, K., Wu, J., Zhang, G., Wang, Z., Fu, L., Tan, H.H., Jagadish, C.: Efficiency enhancement of axial junction InP single nanowire solar cells by dielectric coating. Nano Energy. 28, 106–114: (2016)(a). https://doi.org/10.1016/J.NANOEN.2016.08.032
24. Zhong, Z.Q., Li, Z.Y., Gao, Q., Li, Z., Peng, K., Li, L., Mokkapati, S., Vora, K., Wu, J., Zhang, G.J., Wang, Z.M., Fu, L., Tan, H.H., Jagadish, C.: Efficiency enhancement of axial junction InP single nanowire solar cells by dielectric coating. Nano Energy. **28**, 106–114 (2016). https://doi.org/10.1016/j.nanoen.2016.08.032 )(b).

# Figures

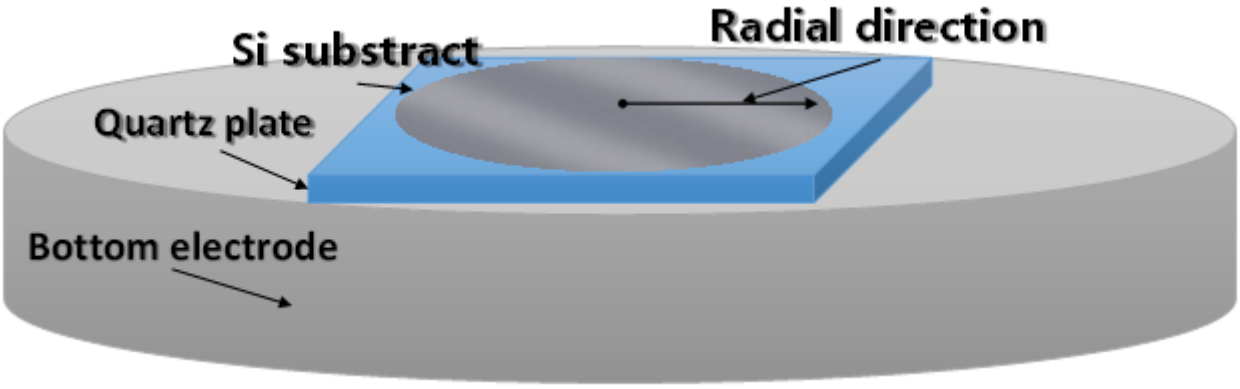


**Figure 1**

Schematic diagram of experimental setup

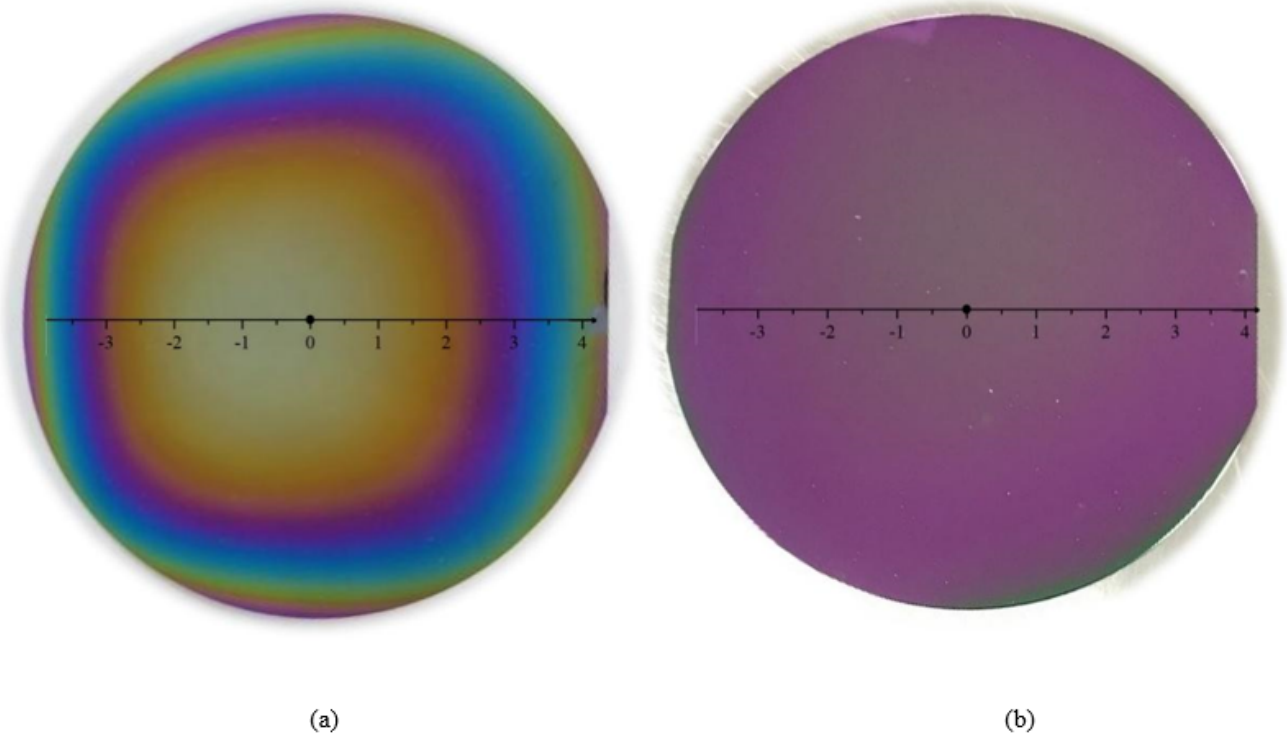


(a) (b)

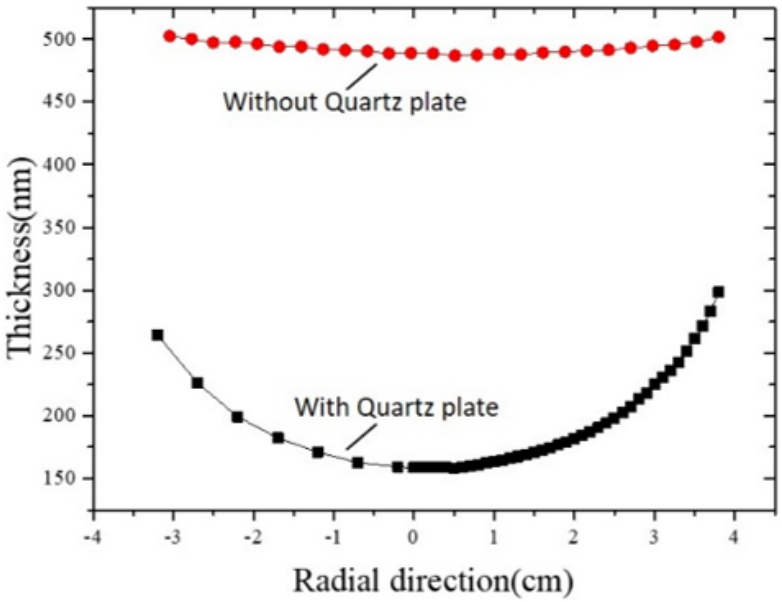


(c)

## Figure 2

(a) The image of SiNx film deposited after introduction of quartz dielectric layer, (b) The image of SiNx deposited without a quartz dielectric layer, (c) Comparison of radial thickness of the above two samples.

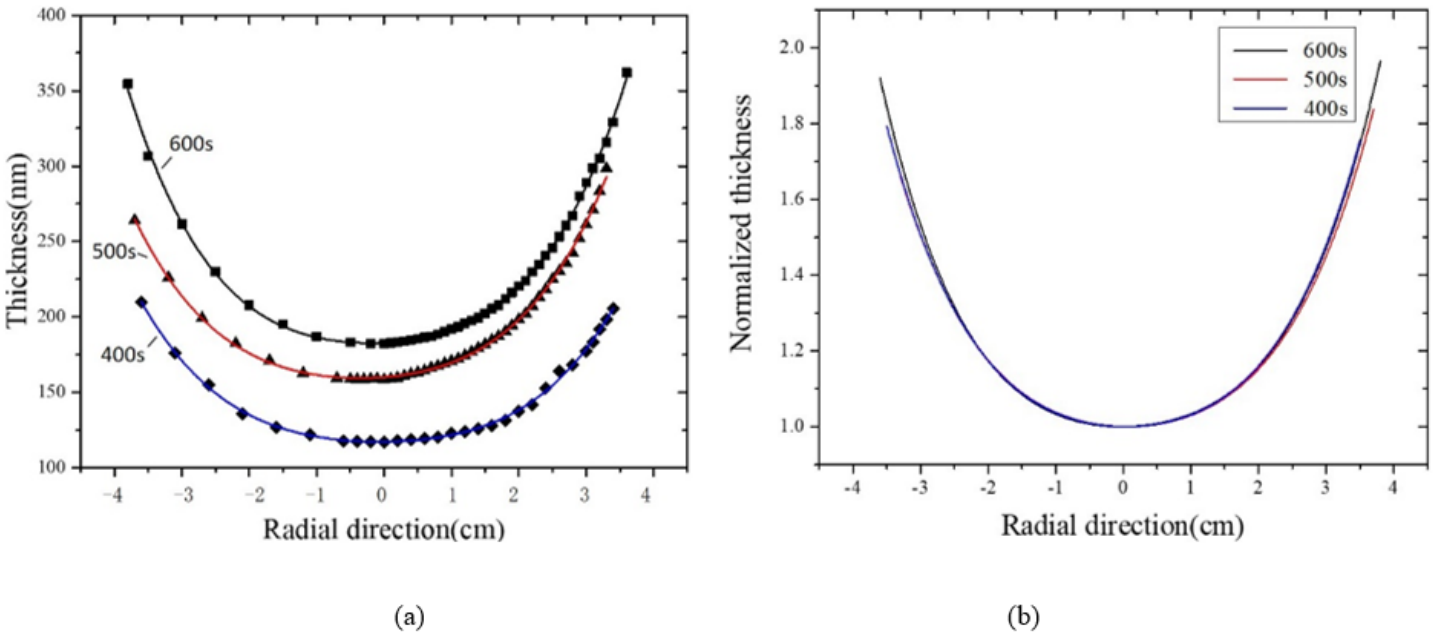


## Figure 3

Radial film thickness distribution curves at different deposition times. (a) Radial distribution curve of actual thickness, (b) Normalized radial thickness distribution curve of thin film.

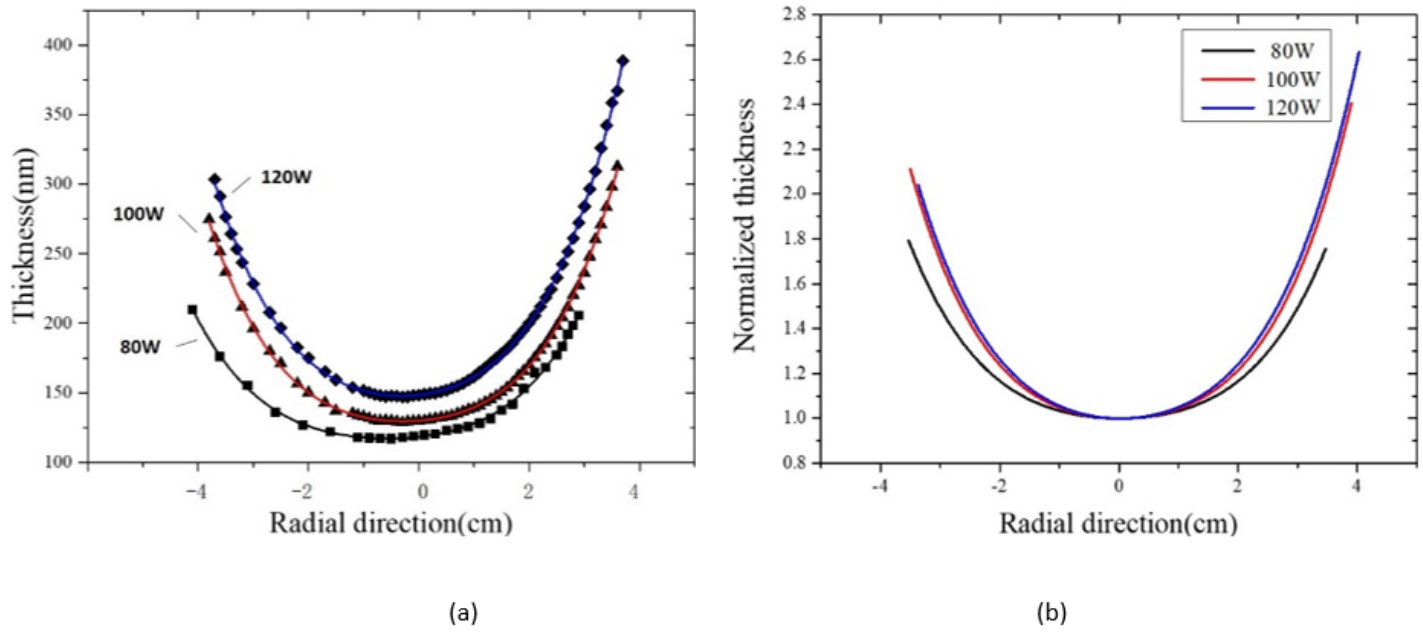


## Figure 4

Thin-film thickness distribution curves of samples processed by different RF powers. (a) Measured radial distribution curve of film thickness, (b) Normalized radial thickness distribution curve of thin film.

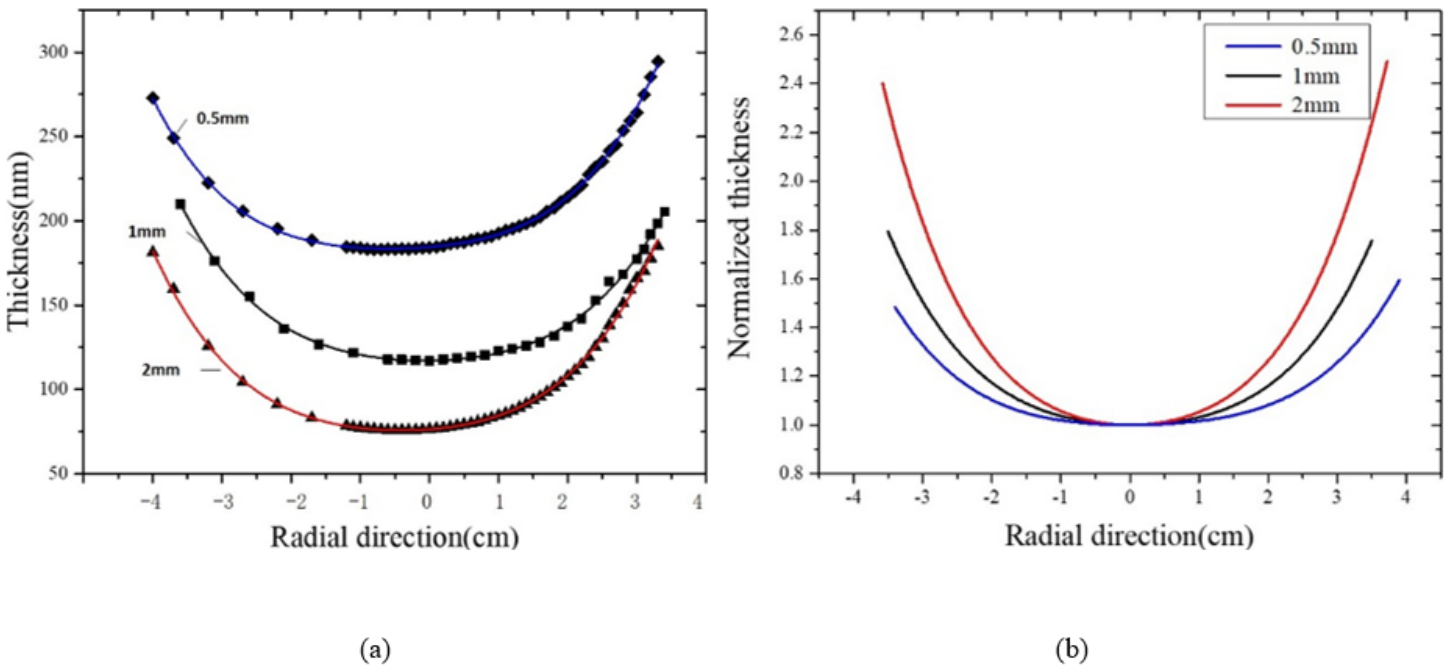


## Figure 5

Thickness distribution curves of films measured by different dielectric layers. (a) Radial distribution curve of actual film thickness, (b) Normalized radial thickness distribution curve of thin film.

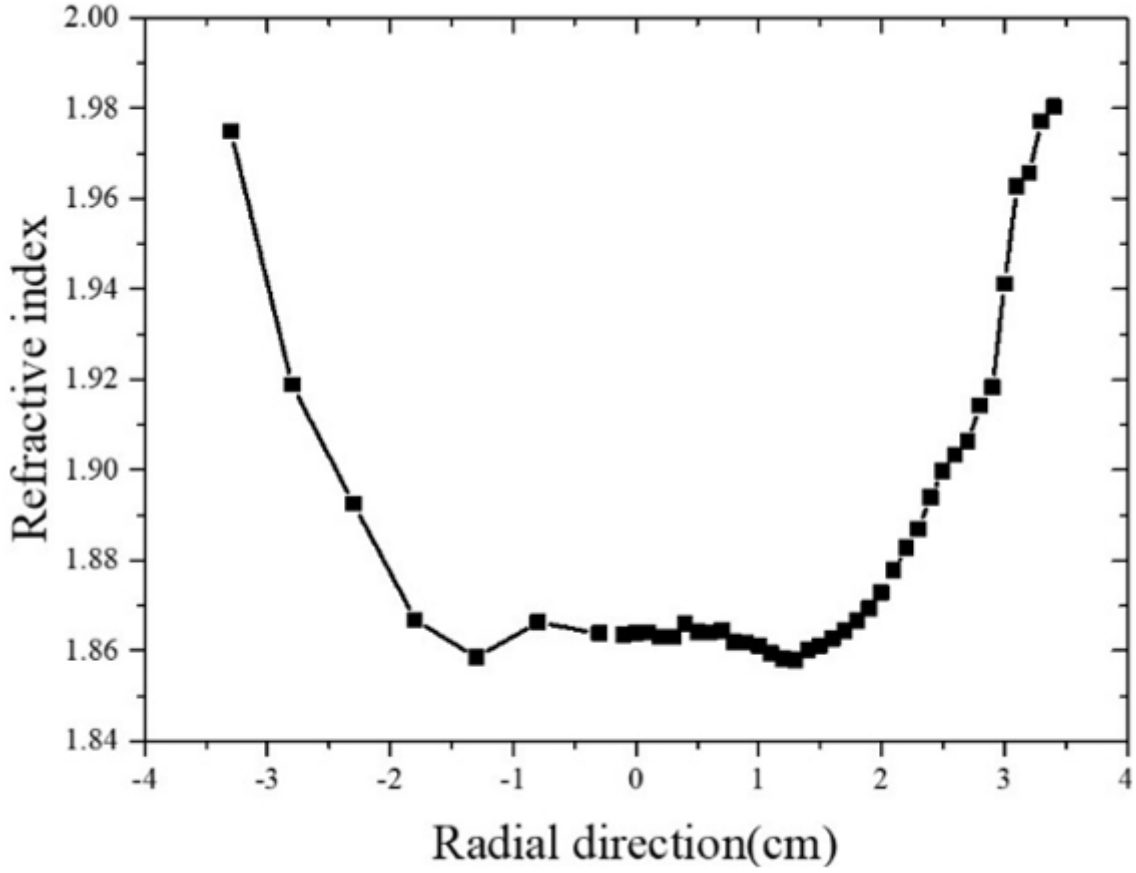

## Figure 6

Radial refractive index distribution curve of SiNx film deposited for 500s.